Theor Chem Acc (2011) 129:141–150
DOI 10.1007/s00214-011-0915-y

REGULAR ARTICLE

Coalescence of metastable states in chemical reactions: double poles of the scattering matrix and exceptional points

Simonetta Cavalli · Dario De Fazio

Received: 3 November 2010 / Accepted: 19 February 2011 / Published online: 12 March 2011

Abstract Accidental degeneracy of two scattering resonances in chemical reactions is discussed. A novel analytical parameterization for the scattering matrix elements valid in the presence of two interacting resonances is derived and applied to investigate the coalescence of metastable states leading to double poles in the partial-wave amplitude. We show how double poles can manifest themselves in reaction cross-sections and discuss their relationship with exceptional points. The presence of two degenerate resonances interacting with each other can create a peculiar double-peak structure in the reaction probability. At the energy where the two decaying states coalesce the scattering matrix has a double pole and correspondingly the reaction probability reaches its minimum value. This novel formula has been tested with the well-established data obtained for the $F + H_2$ reaction, for which previous studies have revealed the existence of two interfering resonance pathways. The good agreement of model predictions and quantum scattering calculations shows that the present approach is reliable. Hence, we claim that it provides a way for the observation of interacting resonances in molecular collisions. Resonance positions and partial widths can be obtained by fitting the numerically calculated state-to-state reaction probabilities to the square modulus of the novel expression for the scattering matrix elements derived in the paper.

S. Cavalli (✉)
Dipartimento di Chimica, Università di Perugia,
06123 Perugia, Italy
e-mail: cavalli@unipg.it

D. De Fazio
Istituto Metodologie Inorganiche e dei Plasmi,
CNR, 00016 Monterotondo, Italy

Keywords Feshbach resonances · Double poles · Accidental degeneracy · Reaction probability · Scattering matrix · Molecular collisions

1 Introduction

In the field of reaction dynamics, the resonance phenomenon is related to the existence of nearly bound states of the reaction complex. The temporary trapping of translational energy in the internal modes of the complex leads to a time-delay for the reactive collision manifesting itself in rapid variations in reaction probabilities and cross-sections. Quantum resonance effects have long been known to occur in chemical reactions, for a review see [1–6], but only recently they have been observed in reactive scattering experiments [7–10]. More subtle quantum effects can also arise for reactions in which two or more regions of trapping are available. In a crossed molecular beam experiment on the $F + H_2$ reaction, Qiu et al. [9] have observed a pronounced forward-scattering peak for the production of the HF molecule in the second vibrational state which, on the base of quantum scattering calculations, has been attributed to the constructive interference between two resonant pathways. For the $H + D_2$ reaction, oscillations have been observed in the experimental differential cross-section for the production of the HD molecule in the ground vibrational state and have been attributed to the interference effects of different quantized transition-state pathways [8].

In this paper, we are concerned with two coupled metastable states of the reaction complex formed in a reactive collision. Focus is on the problem of their accidental degeneracy leading to double poles of the scattering matrix, which, as pointed out in [11–13], are a signature for exceptional points, i.e. points at which a joint crossing of

energies and widths occurs [14, 15]. While two interacting bound states avoid always crossing, for two decaying states which are coupled to each other, a rich phenomenology of crossing and anti-crossing of energies and widths can be observed, in the complex energy plane, as a function of a tuning parameter while keeping constant the interaction between them [11–13, 16–21]. In the last decade, the presence of exceptional points in quantum systems has attracted much interest because of its many applications. For example, very recent studies have shown that they appear in spectra of atoms in external fields [22, 23], in molecular photo-dissociation processes [24, 25] and in laser-assisted electron-atom scattering [26].

For isolated resonances, the poles manifest themselves in reaction probabilities as peaks of Breit–Wigner shape [27]. The case discussed here, in which two simple poles coalesce into a double pole, is more tricky. When two overlapping metastable states interacting with each other occur at the same partial wave two separated peaks can appear in the reaction probability at energies that do not coincide with the resonance positions. At the energy of the double pole, at which the coupled resonance states are at the same energy position and have the same lifetime, the reaction probability exhibits a minimum. We derive an analytical parameterization of the scattering matrix elements valid in the neighborhood of two near degenerate coupled resonances that is capable to account for such a behavior. This novel formula, which depends on six parameters and holds through the double pole, is useful to calculate resonance positions and lifetimes. Namely, these quantities can be estimated by fitting the numerically obtained state-to-state reaction probabilities to the square modulus of the analytical expression for the scattering matrix elements given in the paper. This is an alternative approach to the analysis based on the time-delay matrix or on the numerical reconstruction of the poles of the scattering matrix.

The correctness of the equations given in the paper has been tested with the well-established data for the $F + H_2$ reaction. This reaction has been extensively studied from both the experimentalists and the theoreticians over the last three decades. The $F + H_2$ story has been summarized in many review papers, and we refer those who are interested to [28] and references therein. It has long been known that Feshbach resonances strongly affect the reactive dynamics of this system (for an exhaustive review see [29–34]). In particular, a short-lived resonance in the transition-state region and a long-lived metastable state supported by the van der Waals well in the exit channel have been found to interfere [31–33]. The highly structured angular product distribution affecting the HF products in the second vibrational state was attributed [31–33] to the constructive quantum interference between these two resonant pathways. Subsequently, in order to investigate in more detail the interaction between the two metastable states, we have undertaken a systematic study of the resonance parameters and their dependence on the total angular momentum [35–37]. Some of the quantum structures appearing in the angular product distribution have been observed in molecular beam experiments [9] although at slightly lower energies than theoretically predicted on the base of rigorous quantum scattering calculations [31–33, 35, 36] on the Stark and Werner potential energy surface. Also, the physical origin of both the forward-scattering peak in the angular product distribution and the quantum oscillations in the integral cross-section has been traced using semiclassical complex angular momentum analysis [38, 39]. Moreover, it has been found that the two resonances in question undergo energy crossing and width anti-crossing as a function of the the total angular momentum quantum number [35, 36, 40].

For the reasons illustrated above, the $F + H_2$ reaction provides a good concrete example to assess the accuracy of model calculations and the usefulness of the present formulas to unravel signatures of interacting resonances. Here, we use the numerical values of the resonance energies and lifetimes and of the state-to-state reaction probabilities obtained in previous studies [35, 36] as reference data. The good agreement between the model predictions and the results of rigorous quantum scattering calculations [35, 36] demonstrates that the model is capable to account quantitatively for the quantum effects arising from the coupling between resonance states. Furthermore, we show that fitting the scattering matrix elements calculated numerically or their square modulus, i.e. the state-to-state reaction probabilities, to the corresponding analytic expressions derived in this paper it is possible to estimate not only the complex energies of the resonance poles but also the coupling between them.

In Sect. 2, we apply the non-Hermitian Hamiltonian approach to obtain an analytical expression of the scattering matrix valid in the vicinity of two near degenerate interacting resonances coupled to two open channels. The phenomenon of the coalescence of metastable states and its relation to the occurrence of double poles in the partial-wave amplitude and exceptional points in parameter space are discussed in Sect. 3. The implementation of the present approach to evaluate the resonance energies and widths via the fitting of reaction probabilities is illustrated in Sect. 3.1. Some conclusions will follow in Sect. 4.

2 Interacting scattering resonances

Within the scattering theory [27], resonances are observable manifestations of poles of the scattering matrix, $\boldsymbol{S}$, at the complex energies

$$z_r = E_r - i\Gamma_r/2 \tag{1}$$

where E_r gives the position in energy while the width Γ_r is simply related to the lifetime of the metastable state,

$$\tau = \hbar/\Gamma_r. \tag{2}$$

From another perspective, see for example [18, 19], resonance states have also been seen as the eigenstates of a symmetric non-Hermitian matrix

$$\boldsymbol{\mathcal{H}} = \boldsymbol{H} - \frac{i}{2}\boldsymbol{W}^t\boldsymbol{W} \tag{3}$$

where $\boldsymbol{H}$ is the Hamiltonian matrix of the closed system, while the matrices $\boldsymbol{W}$ and $\boldsymbol{W}^t$ are the decay matrix and its transposed one, respectively.

It has been shown [41] that the poles of $\boldsymbol{S}$ coincide with the complex eigenvalues of $\boldsymbol{\mathcal{H}}$

$$\det(z_r\boldsymbol{I} - \boldsymbol{\mathcal{H}}) = 0 \tag{4}$$

with $\boldsymbol{I}$ being the unity matrix.

The relationship between the two approaches described above is made more transparent by an expression of the scattering matrix

$$\boldsymbol{S}(E,J) = \boldsymbol{U}\Big(\boldsymbol{I} - i\boldsymbol{W}[E\boldsymbol{I} - \boldsymbol{\mathcal{H}}]^{-1}\boldsymbol{W}^t\Big)\boldsymbol{U}^\dagger \tag{5}$$

taken from nuclear physics [42]. Here, E and J denote the total energy and the total angular momentum quantum number, respectively, while the matrix $\boldsymbol{U}$ and its adjoint $\boldsymbol{U}^\dagger$ take into account the background scattering.

The limits of this paper do not allow us to fully illustrate the wide variety of methods that have been developed over the years to calculate resonance energies, lifetimes and cross-sections, and we refer those who wish to gain insight into the nature of reactive scattering resonances to [1] and to [43] for subjects such as complex scaling. For a review of the complex angular momentum poles applications in molecular collisions see [44].

We consider a bimolecular reaction of the type

$$\mathrm{A} + \mathrm{BC}(n) \rightarrow \mathrm{AB}(n') + \mathrm{C}$$

where n and n' denote collectively the vibrational, rotational and helicity quantum numbers for the initial and final states, respectively. At selected E and J, the state-to-state reaction probability

$$P_{nn'}(E,J) = |S_{nn'}|^2 \tag{6}$$

is given by the square modulus of the scattering matrix element. Once we know the scattering matrix elements, the calculation of integral and differential cross-sections for state-to-state transitions is straightforward [27].

Typically, a peak of Breit–Wigner shape in the energy dependence of $P_{nn'}$ is interpreted as a signature of an isolated metastable state produced during the reactive collision. For a chemical reaction whose reaction probability exhibits a characteristic double-peak structure as a function of the collision energy, the interpretation is less intuitive. In the following, we apply the non-Hermitian effective Hamiltonian approach to show that two interacting resonances can account for such a behavior while the results are discussed in Sect. 3.

2.1 S-matrix for a two channel reaction

In this section, a model two channel reaction whose dynamics is dominated by two resonance states is considered. Starting from a general form of the Hamiltonian matrix, we obtain an explicit expression of the scattering matrix valid in the vicinity of two resonances, a and b, coupled to two open channels, n and n'. Being bimolecular reactions time-reversal invariant systems, the $\boldsymbol{S}$-matrix is symmetric other than unitary and the matrices $\boldsymbol{H}$ and $\boldsymbol{W}^t\boldsymbol{W}$ appearing in Eq. 3 are real and symmetric. In this case, all the matrices involved are 2×2 dimensional. The background scattering is assumed to be small and constant in the neighborhood of a resonance state and, in order to make the arguments treated simpler, it is not taken into account. Moreover, we restrict our analysis to an energy region away from thresholds.

The approximations introduced in the model have the advantage of practical convenience. However, they are justified provided that the double resonance region is narrow compared to the energy dependence of direct scattering, so that the effects associated with rapid variation of pure background scattering and interference of background and resonance scattering can be neglected. As discussed by previous workers, see for example [45], the formulas describing single resonances as isolated and narrow should be applied with caution since they do not explain the complicated interplay of all resonances and background terms. The same arguments apply also in the case of the double resonances analyzed in the following.

Let us consider the following general expression for the Hamiltonian matrix in Eq. 3

$$\boldsymbol{\mathcal{H}} = \begin{pmatrix} \epsilon_1 & 0 \\ 0 & \epsilon_2 \end{pmatrix} + \begin{pmatrix} 0 & v \\ v & 0 \end{pmatrix} \tag{7}$$

where ϵ_1 and ϵ_2 are the complex energies of the unperturbed resonance states

$$\begin{aligned} \epsilon_1 &= e_1 - i\gamma_1/2 \\ \epsilon_2 &= e_2 - i\gamma_2/2 \end{aligned} \tag{8}$$

and $v = v_x - iv_y$ is the interaction between them. Here, e_1 and e_2 represent the rotational and vibrational energy of the

metastable levels and γ_1 and γ_2 are the corresponding widths. Since a scattering resonance is due to a reaction complex of the colliding species, both the energies and the widths of metastable states depend on the total angular momentum of the system, see next section.

The eigenvalues of the effective Hamiltonian in Eq. 7 coincide with the poles, z_a and z_b, of the $\boldsymbol{S}$-matrix

$$z_{a,b} = \frac{\epsilon_1 + \epsilon_2}{2} \pm \frac{\sqrt{(\epsilon_1 - \epsilon_2)^2 + 4v^2}}{2} \tag{9}$$

where the discriminant

$$(\epsilon_1 - \epsilon_2)^2 + 4v^2 = d^2 e^{-2i\theta} \tag{10}$$

can be identified with the square of pole separation, $(z_a - z_b) = de^{-i\theta}$, which accordingly depends on J and v. To bring about the degeneracy of a and b states, the variation of both the total angular momentum quantum number and the interaction strength is required.

The partial wave $\boldsymbol{S}$-matrix element connecting channels n and n' is completely defined by six arbitrary parameters which can be chosen in many different ways. In order to make a choice suitable to treat the coalescence of the states a and b in the complex energy plane, we have found it convenient to introduce as new variables: the distance between the poles, d, in the complex energy plane

$$d = \left\{ \left[(e_2 - e_2)^2 - \frac{1}{4}(\gamma_1 - \gamma_2)^2 + 4v_x^2 - 4v_y^2 \right]^2 + 4\left[\frac{1}{2}(\gamma_1 - \gamma_2)(e_1 - e_2) + 4v_x v_y \right]^2 \right\}^{1/4} \tag{11}$$

and the angle, θ, that the direction of d makes with the energy axis

$$\theta = \arctan \times \left(\frac{d^2 - \left[(e_1 - e_2)^2 - \frac{1}{4}(\gamma_1 - \gamma_2)^2 + 4v_x^2 - 4v_y^2 \right]}{d^2 + \left[(e_1 - e_2)^2 + \frac{1}{4}(\gamma_1 - \gamma_2)^2 - 4v_x^2 + 4v_y^2 \right]} \right)^{1/2}, \tag{12}$$

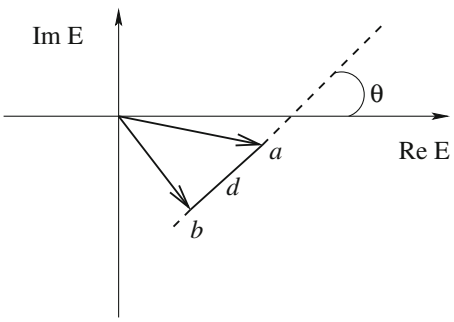

Fig. 1 Schematic representation of two resonance states, a and b, in the complex energy plane. The vector separation between them is characterized by magnitude d and direction θ

see Fig. 1 for a schematic representation of these quantities.

Moreover, it has been shown [46, 47] that through a change of the internal basis, the Hamiltonian matrix in Eq. 7 can be written as

$$\boldsymbol{\mathcal{H}} = \frac{z_a + z_b}{2}\boldsymbol{I} + \frac{e^{-i\theta}}{2}\begin{pmatrix} k\mu - d & i\sqrt{k\mu(k\mu - 2d)} \\ i\sqrt{k\mu(k\mu - 2d)} & -k\mu + d \end{pmatrix} \tag{13}$$

where

$$\begin{aligned} z_a &= E_a - i\frac{\Gamma_a}{2} \\ z_b &= E_b - i\frac{\Gamma_b}{2} \end{aligned} \tag{14}$$

are the complex eigenvalues given in Eq. 9. The parameter μ measures the mixing between resonance states (for details see Eq. 23 below) and the quantity k has been defined as follows:

$$k = d + \sqrt{d^2 + \Gamma_a \Gamma_b}. \tag{15}$$

An explicit expression of the $\boldsymbol{S}$-matrix being strictly unitary and valid through a double pole is obtained inserting Eq. 13 in Eq. 5. In the vicinity of two interacting resonances coupled to two open channels, the partial wave S-matrix element connecting n and n' can be written as

$$S_{nn'} = \delta_{nn'} - \frac{i}{2}\left\{ \frac{(W_{n1}W_{n'1} + W_{n2}W_{n'2})}{E - z_a} + \frac{(W_{n1}W_{n'1} + W_{n2}W_{n'2})}{E - z_b} + e^{-i\theta}\frac{(k\mu - d)(W_{n1}W_{n'1} - W_{n2}W_{n'2}) + i\sqrt{k\mu(k\mu - 2d)}(W_{n1}W_{n'2} + W_{n2}W_{n'1})}{(E - z_a)(E - z_b)} \right\} \tag{16}$$

where the elements of the decay matrix

$$\boldsymbol{W} = \begin{pmatrix} W_{n1} & W_{n2} \\ W_{n'1} & W_{n'2} \end{pmatrix} \tag{17}$$

contain the coupling of the unperturbed states to channels n and n'. We can notice that $\boldsymbol{W}$ is made up of two column vectors, $\vec{W}_1$ and $\vec{W}_2$, each with two elements. From the comparison of Eq. 7 with Eq. 13, we easily find out that these elements must obey the following relations

$$\begin{aligned} \boldsymbol{W}^t\boldsymbol{W} &= \begin{pmatrix} |\vec{W}_1|^2 & \vec{W}_1 \cdot \vec{W}_2 \\ \vec{W}_1 \cdot \vec{W}_2 & |\vec{W}_2|^2 \end{pmatrix} \\ &= \begin{pmatrix} \Gamma + (k\mu - d)\sin\theta & -\sqrt{k\mu(k\mu - 2d)}\cos\theta \\ -\sqrt{k\mu(k\mu - 2d)}\cos\theta & \Gamma - (k\mu - d)\sin\theta \end{pmatrix} \end{aligned} \tag{18}$$

where

$$\Gamma = (\Gamma_a + \Gamma_b)/2 \tag{19}$$

is the total width. It turns out that these constraints fulfill the unitary condition for the scattering matrix as well.

The Cartesian components of $\vec{W}_1$ and $\vec{W}_2$ are real quantities which we parametrize in polar coordinates:

$$\begin{aligned} W_{n1} &= \sqrt{\Gamma + (k\mu - d)\sin\theta}\cos\phi_1 \\ W_{n'1} &= \sqrt{\Gamma + (k\mu - d)\sin\theta}\sin\phi_1 \\ W_{n2} &= \sqrt{\Gamma - (k\mu - d)\sin\theta}\cos\phi_2 \\ W_{n'2} &= \sqrt{\Gamma - (k\mu - d)\sin\theta}\sin\phi_2; \end{aligned} \tag{20}$$

with ϕ_1 and ϕ_2 defining the orientation in channel space of $\vec{W}_1$ and $\vec{W}_2$, respectively. Inserting these definitions into Eq. 16, we express the terms in the numerator as function of the new variables

$$\begin{aligned} W_{n1}W_{n'1} + W_{n2}W_{n'2} &= \Gamma\cos\delta\sin\phi \\ &\quad + (k\mu - d)\sin\theta\sin\delta\cos\phi \\ W_{n1}W_{n'1} - W_{n2}W_{n'2} &= \Gamma\sin\delta\cos\phi \\ &\quad + (k\mu - d)\sin\theta\cos\delta\sin\phi \\ W_{n1}W_{n'2} + W_{n2}W_{n'1} &= \sin\phi\sqrt{\Gamma^2 - (k\mu - d)^2\sin^2\theta} \end{aligned} \tag{21}$$

where $\phi = \phi_1 + \phi_2$ and $\delta = \phi_1 - \phi_2$. We note that being δ the angle included between the vectors $\vec{W}_1$ and $\vec{W}_2$, from Eq. 22 (see below), it is straightforward to show that this angular variable is redundant. Exploiting the properties of the vector product between $\vec{W}_1$ and $\vec{W}_2$

$$\begin{aligned} |\vec{W}_1 \times \vec{W}_2| &= |\vec{W}_1||\vec{W}_2|\sin\delta \\ &= \sqrt{\Gamma^2 + d^2\sin^2\theta - k\mu(k\mu - 2d)} \end{aligned} \tag{22}$$

we easily find out that the variation of the mixing parameter μ is restricted to the range

$$\frac{2d}{k} \le \mu \le 1. \tag{23}$$

The limit of non-interacting resonances is $\mu = 2\ d/k$, where $\vec{W}_1$ and $\vec{W}_2$ are orthogonal. The opposite extreme is $\mu = 1$, where the vectors are parallel and resonance states decay preferentially to the same open channel. The interaction between overlapping resonances occurs via the continuum of the scattering states. From the diagonalization of the effective Hamiltonian in Eq. 7, we find out that the coupling coefficient v is related to the parameter μ through the following relationship

$$|v| = \frac{\sqrt{k\mu(k\mu - 2d)}}{2} \tag{24}$$

where $|v| = \sqrt{v_x^2 + v_y^2}$, with $v_x = |v|\sin\theta$ and $v_y = |v|\cos\theta$.

The relations obtained in Eq. 21 can be used to compute the partial-wave amplitude $S_{nn'}$ as a function of the new variables: d, μ, Γ, $\mathcal{E} = (E_a + E_b)/2$ and the angles θ and ϕ. In particular, when $\mu = 1$, this general expression reads

$$\begin{aligned} S_{nn'} &= \delta_{nn'} + \frac{i\sin\phi}{2} \\ &\quad \times \left\{ \frac{\Gamma_a}{(E - z_a)} + \frac{\Gamma_b}{(E - z_b)} - i\frac{\Gamma_a\Gamma_b}{(E - z_a)(E - z_b)} \right\} \end{aligned} \tag{25}$$

which can be written also as

$$S_{nn'} = \delta_{nn'} + \sin\phi\sin\eta\exp(-i\eta) \tag{26}$$

with η being the phase shift at a given partial wave

$$\eta = \arctan\frac{\Gamma_a/2}{E_a - E} + \arctan\frac{\Gamma_b/2}{E_b - E}. \tag{27}$$

We can see that both poles contribute to the phase shift. Taking the energy-derivative of the phase shift, we easily find out that, in the case of two overlapping resonances decaying to the same open channel, the energy profile of the time-delay is given by the sum of two Lorentzian [35, 36] while, as it is well known, at an isolated resonance, the time-delay shows a Lorentzian like profile [27]. Also, the simple formula in Eq. 27 allows to obtain a parametric expression of the reaction probability

$$P_{nn'} = \sin^2\phi\sin^2\eta \tag{28}$$

which can be used to extract resonance parameters at the degeneracy when only one continuum is considered, see next section.

3 Accidental degeneracy of metastable states

In this section, we discuss the interesting phenomenon of accidental degeneracy of two scattering resonances. For

two interacting resonances in a two box microwave cavity, a rich phenomenology of crossing and anti-crossing of energies and/or widths has been observed experimentally as a function of certain parameters [16, 17]. On the base of the value taken from the coupling strength, three different regimes, denoted as critical, overcritical and subcritical coupling, respectively [11–13, 16–19], have been distinguished. In the first case, a joint crossing of energies and widths is observed. In the second case, the two states repel in energy but align their widths while in the third one they attract in energy but repel in widths. In the following, we apply the analysis developed in [16, 17] to investigate the motion of the poles, z_a and z_b, of the reactive scattering matrix. We show that in a chemical reaction the same phenomenology can be observed varying the mixing between decaying states and the total angular momentum quantum number, this latter acting here as a tuning parameter.

Typically, a slight dependence on J is observed for lifetimes while the energies are more strongly influenced from the rotational modes of the transient species. It has been shown [48] that molecular rotations affect resonance widths at a lower order. Therefore, we assume that the energies of the unperturbed states (see Eq. 8)

$$\begin{aligned} e_1 &= e_1^0 + B_1 J(J+1) \\ e_2 &= e_2^0 + B_2 J(J+1) \end{aligned} \tag{29}$$

increases linearly with $J(J+1)$. Here, B_1 and B_2 are the rotational constants while e_1^0 and e_2^0 denote the energies of the lowest vibrational level. This is equivalent to the assumption that the reaction complexes behave both as rigid symmetric tops. To a first approximation, the widths γ_1 and γ_2 are considered independent on molecular rotation and assumed equal to the values γ_1^0 and γ_2^0, respectively. The unperturbed levels cross freely at the point $J = J_c$, with

$$J_c = \frac{E_2^0 - E_1^0}{B_1 - B_2} - \frac{1}{2} \tag{30}$$

where the approximation $\sqrt{J(J+1)} \simeq J + 1/2$ has been used. At $J = J_c$, the behavior of z_a and z_b depends strongly on the interaction between the resonance states. The phenomenology observed is conveniently described in terms of the distance between the poles and its orientation in the complex energy plane, see Fig. 1. For an application to a specific chemical reaction, see next subsection.

When $|v| = v_c$, with

$$v_c = \frac{|\gamma_2^0 - \gamma_1^0|}{4} \tag{31}$$

the distance d in Eq. 11 vanishes and the eigenvalues become degenerate. The critical values J_c and v_c define an exceptional point [14, 15] in the parameter space. At the exceptional point, not only the eigenvalues but also the eigenfuntions coalesce [49]. Correspondingly, a joint crossing of energies and widths occurs in the complex energy plane and the S-matrix has a double pole.

The explicit expression of $S_{nn'}$ valid in the presence of accidental degeneracy of two metastable states is easily obtained inserting the value $d = 0$ into Eq. 16

$$\begin{aligned} S_{nn'} = \delta_{nn'} - i\Bigg\{ & \frac{W_{n1}W_{n'1} + W_{n2}W_{n'2}}{E - z} \\ & + k\mu e^{-i\theta} \frac{(W_{n1}W_{n'1} - W_{n2}W_{n'2}) + i(W_{n1}W_{n'2} + W_{n2}W_{n'1})}{(E-z)^2} \Bigg\} \end{aligned} \tag{32}$$

with

$$z = \mathcal{E} - \frac{i}{2}\Gamma = \frac{\epsilon_1(J_c) + \epsilon_2(J_c)}{2} \tag{33}$$

being the complex energy of the degenerate states. We notice that the partial-wave amplitude is given by the sum of two terms: the first one is the contribution of the simple pole while the second one is due to the double pole. Therefore, for resonance states coupled to orthogonal channels, $\mu = 2d/k = 0$, the degeneracy leads to a simple pole, a double pole of the scattering matrix appears only for $\mu > 2d/k$. This result is in agreement with [11–13], where it has been shown that the double pole contribution must be always accompanied by the single pole term.

In the particular case in which $\mu = 1$, the expression of the scattering matrix

$$S_{nn'} = \delta_{nn'} + i \sin\phi \left\{ \frac{\Gamma}{(E-z)} - i\frac{\Gamma^2}{2(E-z)^2} \right\} \tag{34}$$

at the double pole is very simple. The interference between the contribution of the single and double pole terms produces in the reaction probability

$$P_{nn'} = \sin^2\phi \frac{(E-\mathcal{E})^2\Gamma^2}{\left[(E-\mathcal{E})^2 + \Gamma^2/4\right]^2} \tag{35}$$

the double-peak structure illustrated in Fig. 2. When the resonances decay to the same open channel, the reaction probability is symmetric: at $E = \mathcal{E}$ it is zero and two peaks of the same height appear at $E = \mathcal{E} \pm \Gamma/2$. The total cross-section can be obtained summing the reaction probability

$$\sigma_{nn'}(E) = \frac{\pi}{k_n^2} \sum_J (2J+1) P_{nn'} \tag{36}$$

over partial waves. For the purpose of comparison, the Lorentzian energy profile of an isolated resonance is also shown (dashed line) in Fig. 2.

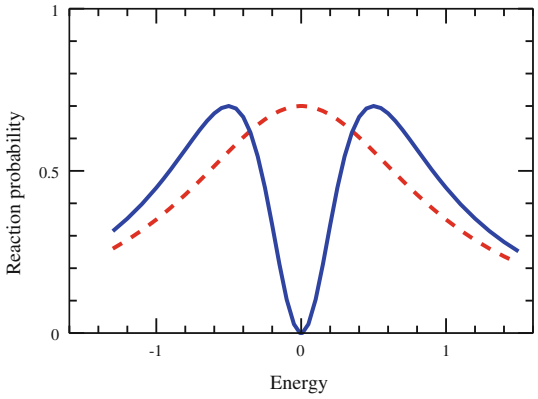

Fig. 2 The reaction probability in the presence of an isolated resonance (*dashed line*) is compared with that for a degenerate doublet of isolated resonances (*solid line*). The energy is dimensionless

In the general case, such a symmetry is broken and the relative height of the two peaks is controlled by the angle θ, see Eq. 12. When $|v| > v_c$, the coupling is referred to as overcritical [16, 17] and, at $J = J_c$, the energy levels avoid crossing while the widths cross. When the coupling is subcritical ($|v| < v_c$), the perturbed energy levels cross freely and the widths avoid crossings without the exchange of the two states at $J = J_c$. These two cases are described setting the angle $\theta = 0$ and $\theta = \pi/2$, respectively. Also, it has been shown [18, 19] that the behavior induced by the imaginary part of the coupling strength differs from that induced by the real part. In the case of overcritical coupling for example, the real part causes the approaching of the lifetimes while the imaginary one causes the formation of different time scales by means of resonance trapping.

3.1 A concrete example: the $F + H_2$ chemical reaction

As briefly summarized in the introduction, the dynamics of the $F + H_2$ reaction is deeply influenced from the presence of two interfering resonance pathways [31–33]. These two states survive in the differential and integral cross-section summation over partial waves and enhance under-barrier reactivity. In the following, we do not aim to further investigate these subjects. Emphasis is placed on the implementation of the fitting procedure for estimating the resonance energy positions and lifetimes. This implementation uses the analytical parameterization of the scattering matrix derived in the previous sections and the well-established data obtained for the benchmark $F + H_2$ reaction in previous quantum scattering calculations [35, 36] carried out on the Stark and Werner potential energy surface [50]. Namely, we consider the short-lived resonance in the transition-state region, labeled as A in [51], and the long-lived metastable state in the exit channel,

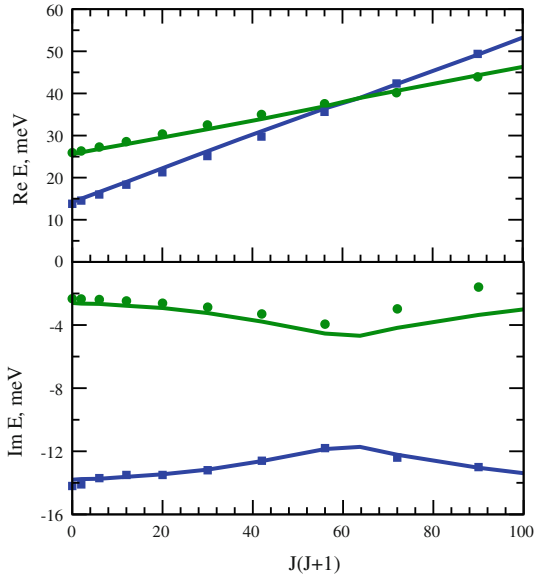

Fig. 3 Energy crossing (*upper panel*) and width attraction (lower panel) for a and b resonances vs $J(J + 1)$ at $|v| = 2.4$ meV. The plots illustrate the comparison of the model prediction (*solid lines*) to the results of quantum scattering calculations (*squares* and *circles* indicate the poles A and B, respectively) carried out for the $F + H_2$ reaction

labeled as B in [51]. These two resonances have been previously analyzed from two main perspectives: one relies on the partial wave analysis of the largest eigenvalue of the collision time-delay matrix [35, 36] while the other one uses the analysis of Regge poles in the complex plane of the total angular momentum [40].

The effective Hamiltonian in Eq. 7 has been diagonalized at several values of the coupling strength. In the calculation of the complex energies of the A and B resonances, we have assumed that the energy levels of the unperturbed states, see Eqs. 8 and 29, shift with J according to

$$\begin{aligned} \epsilon_1 &= 13.8 + 0.4J(J+1) - i7.1 \\ \epsilon_2 &= 25.9 + 0.2J(J+1) - i1.2 \end{aligned} \tag{37}$$

where all the data are expressed in units of meV. The values 0.4 and 0.2 meV, given to the rotational constants B_1 and B_2, are consistent with the molecular structure of the reaction complexes at the saddle point and at the van der Waals equilibrium geometry of the exit channel, respectively [51]. The unperturbed energy positions and widths are set equal to the values calculated at $J = 0$ [35, 36]. The eigenvalues of the effective Hamiltonian calculated at $|v| = 2.4$ meV are shown in Fig. 3. The energy positions (upper panel) and the widths (lower panel) of A and B states are plotted as a function of $J(J + 1)$ for total angular momentum J from 0 to 10. As can be seen in this figure, the values previously obtained from quantum scattering calculations [35, 36] are well reproduced when

we fix the interaction strength, which gives the overlap between the two metastable states, at 2.4 meV. Being this value less than the critical one ($v_c = 2.9$ meV, see Eq. 31), the overlap is not sufficient to produce level repulsion. Therefore, we conclude that this reaction is a case of subcritical coupling, the two resonances cross freely in energy but at the crossing point the states are non-exchanged. The energy of pole A, initially less than that of pole B, moves up faster with total angular momentum and for $J_c = 7.2$ it becomes aligned with B, $E_A = E_B = 38$ meV. A further increase in J moves them apart again, this time the state A lying above the state B. Correspondingly, the widths Γ_A and Γ_B approach each other, and at J_c the width of state A takes its lowest value while the width of state B reaches the maximum value, with $\Gamma_A > \Gamma_B$ in the whole range of J. These findings confirm previous results reported in [35, 36, 38, 40]. For clarity, we note that the eigenvalues of the effective Hamiltonian, denoted as poles A and B, had been labeled as a and b in the previous sections.

The energy profile of the reaction probability for the $F + H_2(v = 0, j = 0) \rightarrow HF(v = 2, j = 0) + H$ reactive transition is plotted in Fig. 4. The plots in the upper panel illustrate the comparison of the model prediction at $J = J_c$ (solid line) with the results of rigorous quantum scattering calculations at $J = 7$ (circles) and $J = 8$ (squares) [35, 36]. The solid line has been calculated using the following expression

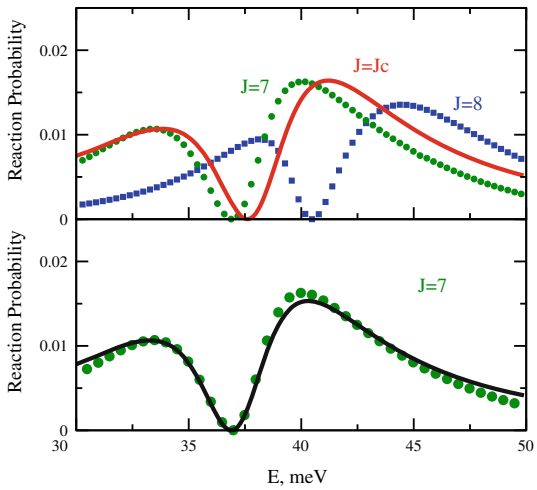

Fig. 4 Energy profile of the reaction probability for the $F + H_2(v = 0, j = 0) \rightarrow HF(v = 2, j = 0) + H$ reactive transition. In the upper panel, the *solid line* has been calculated at $J = J_c$ using Eq. 38 in the main text, while the *circles* and the *squares* have been obtained from rigorous quantum scattering calculation at $J = 7$ (*circles*) and $J = 8$ (*squares*), respectively. In the lower panel, it is shown the fit (*solid line*) of the reaction probability calculated at $J = 7$ to the modulus squared of the general formula for $S_{nn'}$ given in Eq. 16 in the main text

$$P_{nn'} = \frac{\left\{4(k\mu - d)(E - \mathcal{E})\cos\phi + 2\sqrt{k\mu(k\mu - 2d)[\Gamma^2 - (k\mu - d)^2)]}\sin\phi\right\}^2}{[4(E - \mathcal{E})^2 + (\Gamma + d)^2][4(E - \mathcal{E})^2 + (\Gamma^2 - d)]} \tag{38}$$

with n and n' denoting the initial ($v = 0, j = 0$) and final ($v' = 2,\ j' = 0$) scattering channels, respectively. This parametric expression of the reaction probability has been obtained inserting Eqs. 16 into 6 and imposing the constraint that $E_A = E_B$. Therefore, it is valid only at J_c where it is $\theta = \pi/2$. In the calculation of $P_{nn'}$, we have used the following values as input data: $\mu = 0.8$, $\phi = \pi/18$, $d = 3.6$ meV, $\mathcal{E} = 38$ meV and $\Gamma = 8.2$ meV. These values have been calculated from the eigenvalues and the eigenvectors of the effective Hamiltonian at J_c. Moreover, $P_{nn'}$ has been scaled by a constant factor ($c = 0.22$) which takes into account the effective number of open channels coupled to the decaying states. The results illustrated in the upper panel of Fig. 4 demonstrate that the model is capable to account quantitatively for the line shape of the two separated peaks in the energy profile of $P_{nn'}$.

Finally, we show that the resonance positions and widths can be calculated by fitting the energy profile of the reaction probability for each given total angular momentum quantum number to the square modulus of the general formula for $S_{nn'}$ given in Eq. 16. As an illustration of the fit accuracy, the results at $J = 7$ are plotted in the lower panel of Fig. 4. The value of the mixing parameter, $\mu = 0.8$, and of the angle, $\phi = \pi/18$, do not vary with respect to the case where $J = J_c$ while the other parameters ($d = 3.7$ meV, $\mathcal{E} = 37.2$ meV, $\Gamma = 7.9$ meV and $\theta = 0.51\pi$) are slightly different. From this set of data, we find out that $z_a = 37.1 - i5.8$ meV and $z_b = 37.2 - i2.1$ meV. These values are in good agreement with the complex energies obtained from the analysis of the largest eigenvalue, $q_{\max}$, of the time-delay matrix [35, 36] or from the analysis of the Regge poles [40]. Also, with the help of Eq. 24 we estimate

that $v_y = 0.1$ meV and $v_x = 2.1$ meV with $|v| \simeq v_x$. The slight discrepancy between $|v| = 2.1$ meV and the value 2.4 meV (see Fig.3) can be reasonably attributed to the effects of anharmonicity and centrifugal distortion neglected in Eq. 37. For resonance states, these latter are much more pronounced than for most chemically bound species. At $J = 7$, the fitting procedure requires more care than for other values of J because the two resonances are at near degenerate energy positions. Fitting of the same accuracy have been obtained at all partial waves.

As described in [35, 36], the reaction probabilities associated with reactive transitions in the collision energy range of 10–50 meV exhibit two features, separated by a minimum which, at zero total angular momentum, are peaked near the maxima of the spectrum of $q_{\max}$. As J increases, the two peaks get closer and the discrepancy between the maxima of $P_{nn'}$ and the maxima of $q_{\max}$ becomes more evident. At $J = 7$ the two features have a near specular shape, see Fig. 4, but only one maximum, which is peaked where $P_{nn'}$ has a minimum, shows up in the spectrum of $q_{\max}$. The expression of the reaction probability developed here shows that this behavior is general and not limited to the F + H_2 system. According to us, these features can be interpreted as a fingerprint of the contribution of the double pole term in the S-matrix elements (see Eq. 16). In the F + HD reaction, the analogous of resonances A and B appear at higher energies due to zero point effects. Moreover, the energy difference between them is larger so that they do not overlap and appear in the reaction probabilities and cross-sections as isolated resonances [7, 52].

The physical picture emerging from these findings is consistent with previous observations. In [31–33], the authors show that the two resonances in question can be identified as belonging to different wells of an adiabatic potential energy curve correlating to the HF molecule in the third vibrational state. The two resonances are connected by the coupling across the barrier separating their respective wells. When the distance between the poles is larger than the coupling, this latter can be neglected. However, when the levels are nearly aligned, the coupling must be taken into account. As total angular momentum increases, resonance A moves up faster than resonance B and at $J = J_c$ they are aligned but the overlap is not sufficient to produce level repulsion. Therefore, the energy positions of the resonances states cross freely and correspondingly the wide resonance gets narrower while the narrow one gets wider without the exchange of the states after the crossing at J_c. Also, Vanrose [53, 54] has suggested that the interaction between two resonant states in a quantum double-well potential depends on the features of the barrier separating the wells and the double pole marks the transition between the weak coupling (subcritical) and strong coupling (overcritical) cases leading to resonant tunneling and level repulsion regimes, respectively.

4 Conclusions

The non-Hermitian effective Hamiltonian approach has been used to derive an analytical parameterization of the scattering matrix, which is strictly unitary and valid in the neighborhood of two overlapping metastable states whose interaction can lead to the appearance of double poles in the reactive partial-wave amplitude. In order to do so, we have taken into account the interaction between two resonance states via a direct coupling and via the continuum of decay channels. Also, we have shown that this novel parameterization of the scattering matrix elements can be easily implemented to calculate the complex energies of the resonance poles and the coupling between them.

Interference structures caused by overlapping resonance states have been discussed for many years. Molecular rotations and overlap can induce changes on both the lifetimes and the energies of resonance states that cause quantum oscillating structures superimposed to the direct scattering contribution. In this paper, we have provided an expression of the reaction probability depending explicitly on the overlap between metastable states. It has been shown that the coupling can cause the separation of the peaks in the reaction probability, so that their positions do not coincide with the resonance energies and the reaction probability nearly vanishes just at the energy where the energy positions of the two resonances coalesce. Moreover, the analysis of the motion of the poles as a function of the coupling strength and of a tuning parameter, which we have identified in the total angular momentum quantum number in the application to chemical reactions, has contributed to clarify the relationship between double poles of the reactive scattering matrix and exceptional points.

The formulas derived in the paper have been tested on the F + H_2 reaction. The agreement of the model prediction to previous quantum scattering calculations has allowed to assess the utility of our approach to unravel signatures of the interaction between metastable states in scattering observables. This reaction has been so heavily studied that it is almost impossible to produce new insight. However, there is an aspect, emphasized in the paper, that was unknown to us. Within the framework of the present approach, we have shown that this reaction is an example of quantum system with subcritical coupling. The resonance energy crossing and width anti-crossing observed as functions of the total angular momentum quantum number is a general phenomenology observable for all quantum systems with two coupled metastable states whose mixing parameter is lower than a critical value.

Finally, we believe that the formalism presented in this paper could provide a way for the observation of interacting resonances in the future.

Acknowledgments The authors are grateful to V. Aquilanti for stimulating discussions. The authors thank the Italian MIUR for PRIN contracts and the High Performance Computing center at CINECA for computer time awarded via the 'Progetto di Supercalcolo per la Fisica della Materia' Convenzione CINECA-INFM-CNR. D. De F. acknowledges the HPC-EUROPA2 for funding the project number 228398, with the support of the European Community—Research Infrastructure Action of the FP7—and the Barcelona Supercomputing Center (BSC) for the hospitality.

References

1. Fernández-Alonso F, Zare RN (2002) Annu Rev Phys Chem 53:67–99
2. Althorpe SC, Clary DC (2003) Annu Rev Phys Chem 54:493–529
3. Friedman RS, Truhlar DG (1997) In: Truhlar DG, Simon B (eds) Multiparticle quantum scattering with applications to nuclear, atomic, and molecular physics. Springer, New York, pp 243–281
4. Schatz GC (2000) Sci Agric 288:1599–1600
5. Liu K (2001) Annu Rev Phys Chem 52:139–164
6. Yang X (2007) Annu Rev Phys Chem 58:433–459
7. Skodje RT, Skouteris D, Manolopoulos DE, Lee S-H, Dong F, Liu K (2000) J Chem Phys 112:4536
8. Dai D, Wang CC, Harich SA, Wang X, Yang X, Chao SD, Skodje RT (2003) Sci Agric 300:1730–1734
9. Qiu M et al (2006) Sci Agric 311:1440–1443
10. Dong W, Xiao C, Wang T, Dai D, Yang X, Zhang DH (2010) Sci Agric 327:1501–1502
11. Hernández E, Mondragón A (1993) J Phys A Math Gen 26:5595–5611
12. Hernández E, Jáuregui A, Mondragón A (2003) Phys Rev A 67:022721
13. Hernández E, Jáuregui A, Mondragón A (2007) Int J Theor Phys 46:1666–1701
14. Heiss WD (1999) Eur Phys J D 7:1–4
15. Heiss WD, Harney HL (2001) Eur Phys J 17:149–151
16. Philipp M, von Brentano P, Pascovici G, Richter A (2000) Phys Rev E 62:1922–1926
17. Dembowski C, Gräf H-D, Harney HL, Heine A, Heiss WD, Rehfeld H, Richter A (2003) Phys Rev Lett 90:034101
18. Rotter I (1995) Phys Rev E 52:5961–5973
19. Rotter I (2002) Phys Rev E 65:026217
20. Estrada H, Cederbaum LS, Domcke WJ (1986) J Chem Phys 84:152–169
21. Klaiman S, Cederbaum LS (2008) Phys Rev A 78:062113(1–8)
22. Cartarius H, Main J, Wunner G (2007) Phys Rev Lett 99:173003
23. Cartarius H, Main J, Wunner G (2009) Phys Rev A 79:053408
24. Lefebvre R, Atabek O, Sindelka M, Moiseyev N (2009) Phys Rev Lett 103:123003
25. Lefebvre R, Atabek O (2010) Eur Phys J D 56:317–324
26. Kylstra NJ, Joachain CJ (1998) Phys Rev A 57:412–431
27. Taylor JR (1972) Scattering theory. Wiley, New York
28. Hu W, Schatz GC (2006) J Chem Phys 125:132301 and references therein
29. Mielke SL, Lynch GC, Thrular DG, Schwenke DW (1993) Chem Phys Lett 231:10–19
30. Manolopoulos DE (1997) J Chem Soc Faraday Trans 93:673 and references therein
31. Chao SD, Skodje RT (2000) J Chem Phys 113:3487
32. Chao SD, Skodje RT (2002) Theor Chem Acc 108:273–285
33. Chao SD, Skodje RT (2003) J Chem Phys 119:1462–1472
34. Liu K (2006) J Chem Phys 125:32307 and references therein
35. Cavalli S, De Fazio D (2007) Phys Scr 76:C21–C27
36. Aquilanti V, Cavalli S, Simoni A, Aguilar A, Lucas JM, De Fazio D (2004) J Chem Phys 121:11675–11690
37. Aquilanti V, Cavalli S, De Fazio D, Simoni A, Tscherbul TV (2005) J Chem Phys 123:054314
38. Sokolovski D, De Fazio D, Cavalli S, Aquilanti V (2007) J Chem Phys 126:121101
39. Sokolovski D, De Fazio D, Cavalli S, Aquilanti V (2007) Phys Chem Chem Phys 9:5664–5671
40. Sokolovski D, Sen SK, Aquilanti V, Cavalli S, De Fazio D (2007) J Chem Phys 126:084305
41. Rotter I (2003) Phys Rev E 67:026204
42. Verbaarschot JJM, Weidenmüller HA, Zimbauer MR (1985) Phys Rep 129:367–438
43. Moiseyev N (1998) Phys Rep 302:211–293
44. Connor JNL (1990) J Chem Soc Faraday Trans 86:1627–1640
45. Schwenke DW, Truhlar DG (1987) J Chem Phys 87:1095–1106
46. Kumar S (1972) Phys Rev D 5:2128–2130
47. Rebbi C, Slanski R (1970) Phys Rev D 1:1499–1500
48. Sepulchre JA, Gaspard P (1995) J Chem Phys 102:6727–6734
49. Heiss WD, Harney HL (2001) Eur Phys J D 17:149–151
50. Stark K, Werner H-J (1996) J Chem Phys 104:6515–6530
51. Castillo JF, Manolopoulos DE, Stark K, Werner H-J (1996) J Chem Phys 104:6531–6546
52. De Fazio D, Cavalli S, Aquilanti V, Buchachenko AA, Tscherbul TV (2007) J Phys Chem 111:12538–12549
53. Vanrose W (2001) Phys Rev A 64:062708
54. Vanroose W, Van Leuvenz P, Arickxy F, Broeckhove J (1997) J Phys A 30:5543